

Chapter 1

Transport and the first passage time problem with application to cold atoms in optical traps

Eli Barkai, David A. Kessler

*Department of Physics
Institute of Nanotechnology and Advanced Materials
Bar-Ilan University, Ramat-Gan 52900, Israel*

Measurements of spatial diffusion of cold atoms in optical lattices have revealed anomalous super-diffusion, which is controlled by the depth of the optical lattice. We use first passage time statistics to derive the diffusion front of the atoms. In particular, the distributions of areas swept under the first passage curve till its first arrival, and of areas under the Bessel excursion are shown to be powerful tools in the analysis of the atomic cloud. A rather general relation between first passage time statistics and diffusivity is discussed, showing that first passage time analysis is a useful tool in the calculation of transport coefficients. A brief introduction to the semi-classical description of Sisyphus cooling is provided which yields a rich phase diagram for the dynamics.

1. Introduction

Fick's second law predicts how diffusion causes concentration to change in time. Instead of concentration we will use a probability density in one dimension $P(x, t)$ and then Fick's law reads

$$\frac{\partial P}{\partial t} = K_2 \frac{\partial^2 P}{\partial x^2} \quad (1)$$

where K_2 is the diffusion coefficient. For an open system, and particles initially localized at the origin, the solution is a spreading Gaussian packet, with a width proportional to time:

$$\langle x^2 \rangle = 2K_2 t. \quad (2)$$

Such normal diffusion is ubiquitous, which is hardly surprising since the diffusion is merely a sum of random displacements with zero mean. Hence,

following the central limit theorem we expect to find in experiment a Gaussian distribution for the particle position. The Gaussian universality of diffusion processes leaves us with one difficult task, and that is to compute the diffusion constant K_2 . This constant is non-universal, unlike the nearly universal shape of the Gaussian probability packet. Still, non-equilibrium statistical mechanics gives us a recipe (in principle) for the calculation of K_2 which is the famous Green-Kubo formula

$$K_2 = \int_0^\infty d\tau \langle p(t+\tau)p(t) \rangle / m^2 \quad (3)$$

where m is the mass of the particle. This relation between the momentum correlation function and the diffusivity is extensively used in the context of hard and soft condensed matter. The correlation function and the underlying process itself is assumed to be stationary so $\langle p(t+\tau)p(t) \rangle$ is independent of t . The Green-Kubo formula is important since once we obtain the diffusivity of a system we also know its mobility. This is made possible via linear response theory and the well-known Einstein relation which connects the diffusivity with the mobility via the thermal scale $k_b T$ where T is temperature.

All this was established a long time ago, so it is not surprising that physicists have turned their focus to problems that violate this normal behavior. One example is the diffusion and transport of atoms in optical molasses driven by counter propagating laser beams.¹ This system has attracted considerable attention, both for applied purposes like cooling and control of atoms and from a more fundamental point of view, since it exhibits unusual friction and in some cases large deviations from ordinary statistical mechanics. Indeed laser cooling is today the tool of choice in many laboratories which investigate low temperature physics. So basic understanding of statistical properties of laser cooled atoms is a timely subject.

Within the semi-classical picture of Sisyphus cooling, the atoms are subject to a velocity dependent friction force, $F(v)$, defined more precisely below. At low velocities, $F(v) \propto -v$, which is of course normal in the sense that it mimics Stoke's friction for a macroscopic Brownian particle in a viscous medium at room temperatures. Such a friction force is intuitive since it indicates that the faster the particle moves the more energy it dissipates to the surrounding bath. The large v behavior of the atomic friction on the other hand is counterintuitive: it decreases with velocity, $F(v) \sim -1/v$, thus when $v \rightarrow \infty$ the system becomes frictionless. Such a system can be called asymptotically dissipationless, and it exhibits physical

*Transport and the first passage time problem with application to cold atoms in optical traps*³

behaviors very different than standard systems such as non-dissipative ones and systems with kinetic dissipation which does not vanish at high speeds.

This behavior of the friction force is due to the fact that the laser cooling is not effective beyond some critical velocity. Briefly, the effect is caused since a fast particle cannot distinguish the uphill from the downhill in the spatially periodic optical lattice; hence the Sisyphus mechanism which favors the loss of energy when the particle is close to the maximum of the periodic lattice is not effective (see Fig. 1 and caption). Since the friction is vanishingly small for large velocities the equilibrium distribution of the velocities can be shown to obey power law statistics (see details below), and so various average quantities are dominated by fast particles (compared for example with the Maxwellian distribution which is Gaussian). More generally, the kinetics and equilibrium properties of atoms under laser cooling are far from standard: anomalous diffusion, non Gibbsian states, etc. can be found not only in Sisyphus cooling but also in other cooling approaches like sub-recoil laser cooling,² and in Doppler cooling as well.

Indeed in the closing paragraph of Cohen-Tannoudji's Nobel lecture³ he writes "It is clear finally that all the developments which have occurred in the field of laser cooling and trapping are strengthening the connections which can be established between atomic physics and other branches of physics such as condensed matter or statistical physics. The use of Lévy statistics for analyzing sub-recoil cooling is an example of such a fruitful dialogue". Here such a dialogue is extended to the popular Sisyphus cooling mechanism. Lévy statistics roughly refers to power law distributions, which violate the conditions leading to the Gaussian central limit theorem. An example of this is found in a recent experiment performed at the Weizmann Institute.

1.1. *Spatial diffusion of cold atoms*

There, Sagi, et al.⁴ measured the diffusion of ultra-cold ⁸⁷Rb atoms in a one dimensional optical lattice. Starting with a very narrow atomic cloud they recorded the time evolution of the density of the particles, here denoted $P(x, t)$ (normalized to unity). Their work employed the well-known Sisyphus cooling scheme.⁵ As predicted theoretically by Marksteiner, et al.,⁶ the diffusion of the atoms was not Gaussian, so that the assumption that the diffusion process obeys the standard central limit theorem is not valid in this case. We recently determined the precise nature of the non-equilibrium spreading of the atoms, in particular the dynamical

phase diagram of the various different types of behaviors exhibited as the depth of the optical potential is varied, at least within the semiclassical approach.

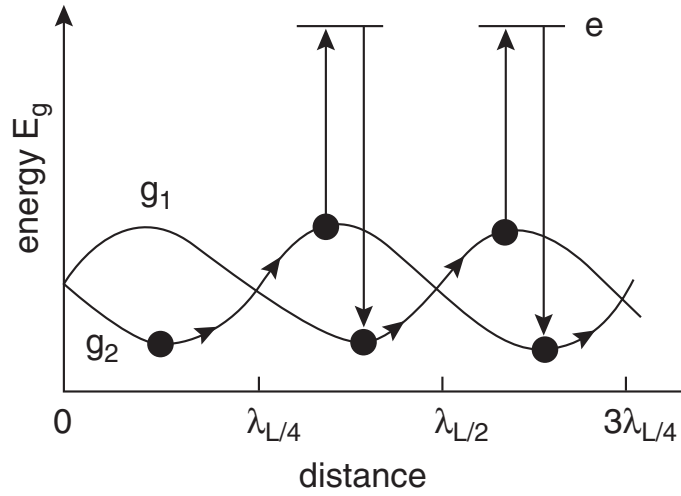


Fig. 1. Sisyphus was punished by Greek gods to push a heavy stone uphill just to have it roll back to its starting point. In Sisyphus cooling, an atom will go up a potential hill created by laser fields, and then falls down to the local ground state, thus losing energy. Such a scheme is made possible only when transitions from the potential maximum to minimum are statistically preferred, which in turn is made possible by clever quantum mechanics, and polarization fields (which control the transitions) which are periodic function of distance specially designed to correspond to the spatial modulation of the energy surfaces (the period is determined by the wavelength of the laser field, λ_L). However, if Sisyphus runs like a bolt, over the hills and the valleys he can fool the gods. Namely Greek gods cannot push him down from the top of the hills, since they need some finite time to implement his punishment. This corresponds to a fast atom whose transitions are not synchronized with it being on maximum of energy surface. So for fast particles, the Sisyphus friction becomes small and decreases, according to the detailed calculations, like $F(v) \propto -1/v$. For more on Sisyphus cooling see.¹

In Ref. 4, the anomalous diffusion data was compared to the solutions of the fractional diffusion equation⁷⁻⁹

$$\frac{\partial^\beta P(x,t)}{\partial t^\beta} = K_\nu \nabla^\nu P(x,t), \quad (4)$$

with $\beta = 1$, so that the time derivative on the left hand side is a first-order derivative. The fractional space derivative on the right hand side is a Weyl-Rietz fractional derivative,⁹ defined below. Here the anomalous

diffusion coefficient K_ν has units cm^ν/sec . A fundamental challenge is to derive such fractional equations from a microscopic theory, without invoking power-law statistics in the first place. Furthermore, the solutions of such equations exhibit a diverging mean-square displacement $\langle x^2 \rangle = \infty$, which violates the principle of causality^a, which restricts physical phenomena to spread at finite speeds. So how can fractional equations like Eq. (4) describe physical reality? We will address this paradox in this work. The solution of Eq. (4) for an initial narrow cloud is given in terms of a Lévy distribution (see details below). The Lévy distribution generalizes the Gaussian distribution in the mathematical problem of the sum of a large number of independent random variables symmetrically distributed about 0, in the case where the variance of the summands diverges, corresponding physically to scale free systems. Here our aim is to derive Lévy statistics and the fractional diffusion equation from the semi-classical picture of Sisyphus cooling. Specifically, we will show that $\beta = 1$ and relate the value of the exponent ν to the depth of the optical lattice U_0 , deriving an expression for the constant K_ν . Furthermore, we discuss the limitations of the fractional framework, and show that for a critical value of the depth of the optical lattice, the dynamics switches to a non-Lévy behavior (i.e. a regime where Eq. (4) is not valid); instead it is related to Richardson-Obukhov diffusion found in turbulence. Thus the semiclassical picture predicts a rich phase diagram for the atomistic diffusion process. We will then compare the results of this analysis to the experimental findings, and see that there are still unresolved discrepancies between the experiment and the theory. Reconciling the two thus poses a major challenge for the future.

Since usual approaches to diffusion, namely Fick's second law and the Green-Kubo formula break down for the case of interest, we cannot use ordinary approaches. Here the power of first passage time statistics enters. We will show how analysis of first passage time statistics yields the diffusion front of a packet of particles. In essence the first passage time tool replaces the failing Green Kubo formula, and leads us to the solution of the problem, namely the exponents β and ν as well as the generalized diffusion constant K_ν . But this is a long journey, so first let us briefly review the concept of Brownian excursions, first passage times for simple Brownian motion, and the distribution of the area swept under Brownian motion till its first passage.

^aSee the discussion in Ref. 10 where the unphysical nature of Lévy flights is discussed and the resolution in terms of Lévy walks is addressed.

1.2. *Brief Survey: Joint PDF for first passage time and the area swept under Brownian motion*

Consider a Brownian motion in one dimension. The time τ_f it takes the particle starting at $x = \epsilon > 0$ to reach $x = 0$ for the first time is the first passage time. The distribution of τ_f has been well investigated both for Brownian motion and for other types of random walks.^{11,12} A quantity which until recently was only of mathematical interest is the total area under the Brownian path in the time interval $(0, \tau_f)$, which was treated by Kearney and Majumdar.¹³ This area, which we denote χ_f , is obviously positive if we start at $x = \epsilon > 0$. Later we will take $\epsilon \rightarrow 0$ which is a subtle point, but for now we keep ϵ finite. The pair of random quantities χ_f and τ_f are clearly correlated since a large τ_f implies statistically a large χ_f . The joint probability density function is denoted as $P(\tau_f, \chi_f)$. Using Bayes' law we may write this density as

$$\psi(\tau_f, \chi_f) = g(\tau_f)P(\chi_f|\tau_f) \quad (5)$$

where $g(\tau_f)$ is the first passage time probability density function (PDF), which at least for Brownian motion is well investigated. In particular, $g(\tau_f)$ decays as a power for large τ_f ,

$$g(\tau_f) \propto (\tau_f)^{-3/2}, \quad (6)$$

so that the average first passage time, $\langle \tau_f \rangle = \infty$, diverges for one dimensional Brownian motion on the infinite line. $P(\chi_f|\tau_f)$ is the conditional probability density function of χ_f given some fixed τ_f . This leads us to the concept of a Brownian excursion.

A Brownian excursion is a conditioned one dimensional Brownian motion $x(t)$ over the time interval $0 \leq t \leq \tau_f$ (recall here τ_f is fixed to a specific value). The motion starts at $x(0) = \epsilon > 0$, $\epsilon \ll 1$, and ends at $x(\tau_f) = 0$ and is constrained not to cross the origin $x = 0$ in the observation time $(0, \tau_f)$, namely the Brownian excursion is always positive. The area under the Brownian excursion is the object of interest since that gives the conditional probability density $P(\chi_f|\tau_f)$. Thus the statistics of the area under the Brownian excursion also gives the joint PDF of the first passage time and the total area under the Brownian motion.

The area under the Brownian excursion was treated by mathematicians with applications in computer science and graph theory and more recently in the physical context of fluctuations of interfaces.^{14,15} Majumdar and Comtet¹⁵ give a concise introduction and derivation of the solution to this problem in terms of the Airy distribution. We shall soon show that the

*Transport and the first passage time problem with application to cold atoms in optical traps*⁷

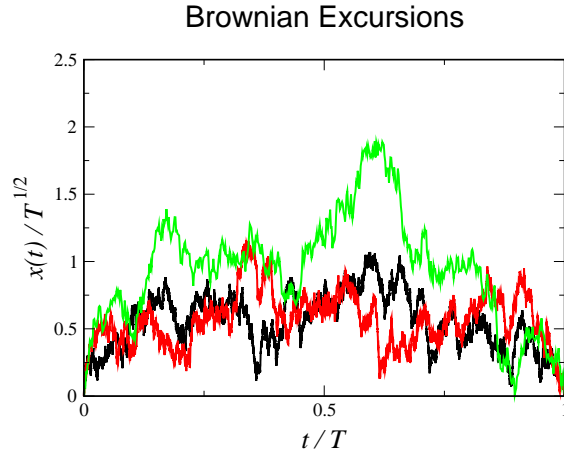


Fig. 2. An example of a Brownian excursion $x(t)$, which in the text is generalized to a Langevin excursion in momentum space, $p(t')$. These are random curves which start and end close to the origin and remain positive for a fixed time. Surprisingly the random area under these curves has started to attract physical attention in diverse problems ranging from fluctuating interfaces and as we show here diffusion of atoms in optical lattices. A related problem is the Tracy-Widom distribution.

solution of the dynamics of the atomic packet demands the solution of a first passage time in momentum space, and the distribution of the area under the random first passage time curve. Thus the random area under a random curve terminated at its first passage turns into a relevant problem, but, fortunately or unfortunately, the apposite curve is not a simple Brownian one.

So, for perspective, we first review what is known about the distribution of A , the random area under the Brownian excursion, $A = \int_0^{\tau_f} x(t)dt$ in the $\epsilon \rightarrow 0$ limit. Since Brownian motion scales like $x \sim t^{1/2}$ the area A scales like $\int_0^{\tau_f} x(t)dt \propto (\tau_f)^{3/2}$. Thus the distribution has the scaling behavior $P_{\tau_f}(A) = (\tau_f)^{-3/2} f(A/(\tau_f)^{3/2})$, where the $(\tau_f)^{-3/2}$ prefactor stems from the normalization condition. The Laplace $x \rightarrow u$ transform of $f(x)$, $\hat{f}(u)$ was computed by Darling and Louchard^{16,17}

$$\hat{f}(u) = u\sqrt{2\pi} \sum_{k=1}^{\infty} \exp\left(-\alpha_k u^{2/3} 2^{-1/3}\right) \quad (7)$$

(here, the diffusion constant of the Brownian motion, arising from the simple random walk used to model the motion, is $1/2$). The α_k 's are the magnitudes of the zeros of the Airy function $Ai(z)$ on the negative real axis $\alpha_1 = 2.3381..$, $\alpha_2 = 4.0879..$, $\alpha_3 = 5.5205..$ and for that reason the distribution is called the Airy distribution. Takács¹⁸ inverted the Laplace transform to find

$$f(x) = \frac{2\sqrt{6}}{x^{10/3}} \sum_{k=1}^{\infty} e^{-b_k/x^2} b_k^{2/3} U(-5/6, 4/3, b_k/x^2) \quad (8)$$

where $b_k = 2(\alpha_k)^3/27$ and $U(a, b, z)$ is the confluent hypergeometric function.¹⁹ Moments and asymptotic behaviors of the Airy distribution can be found in Ref. 15. The function can be calculated and plotted by truncating the sum at some x dependent value.

From this, we can deduce the power law exponent describing the tail of the PDF of the area swept under the Brownian curve till its first passage event $q(\chi_f)$, averaged over all τ_f . Clearly the marginal PDF $q(\chi_f)$ is found from the joint PDF in the usual way by integration

$$q(\chi_f) = \int_0^{\infty} g(\tau_f) P(\chi_f|\tau_f) d\tau_f \quad (9)$$

Using Eq. (6) and the scaling behavior of the conditional PDF $P(\chi_f|\tau_f)$, we have

$$q(\chi_f) \propto \int_0^{\infty} (\tau_f)^{-3/2} (\tau_f)^{-3/2} f(\chi_f/(\tau_f)^{3/2}) d\tau_f. \quad (10)$$

Changing integration variables to $y \equiv \tau_f/(\chi_f)^{2/3}$ we get the asymptotic form

$$q(\chi_f) \propto (\chi_f)^{-4/3}. \quad (11)$$

We see that the scaling exponent $3/2$ for $g(\tau)$ and $4/3$ for $q(\chi_f)$ are easy to obtain and are both related to the scaling of Brownian motion $x \propto t^{1/2}$. The full distribution of $q(\chi_f)$ was recently found by Kearney and Majumdar for finite ϵ . We will later deal with such a calculation in more rigor, but for now we just focus on the exponents. We now turn to showing how the generalization of these concepts lead to the description of the dynamics of cold atoms.

2. Model and Goal

We wish to investigate the spatial density of the atoms, $P(x, t)$. The trajectory of a single particle is $x(t) = \int_0^t p(t) dt/m$ where $p(t)$ is its momentum.

Within the standard picture^{5,6} of Sisyphus cooling, two competing mechanisms describe the dynamics. The cooling force

$$F(p) = -\bar{\alpha}p/[1 + (p/p_c)^2] \quad (12)$$

acts to restore the momentum to the minimum energy state $p = 0$. Momentum diffusion is governed by a diffusion coefficient which is momentum dependent, $D(p) = D_1 + D_2/[1 + (p/p_c)^2]$. The latter describes momentum fluctuations which lead to heating (due to random emission events). We use dimensionless units, time $t \rightarrow t\bar{\alpha}$, momentum $p \rightarrow p/p_c$, the momentum diffusion constant $D = D_1/(p_c)^2\bar{\alpha}$ and $x \rightarrow xm\bar{\alpha}/p_c$. For simplicity, we set $D_2 = 0$ since it does not modify the asymptotic $|p| \rightarrow \infty$ behavior of the diffusive heating term, nor that of the force, and therefore does not modify our main conclusions. The Langevin equations

$$\frac{dp}{dt} = F(p) + \sqrt{2D}\xi(t), \quad (13a)$$

$$\frac{dx}{dt} = p \quad (13b)$$

describe the dynamics in phase space. Here the noise term is Gaussian, has zero mean and is white $\langle \xi(t)\xi(t') \rangle = \delta(t - t')$. The now dimensionless cooling force is

$$F(p) = -\frac{p}{1 + p^2}. \quad (14)$$

The stochastic Eq. (13) give the trajectories of the standard Kramers picture for the semi-classical dynamics in the optical lattice which in turn was derived from microscopical considerations.^{5,6} From the semiclassical treatment of the interaction of the atoms with the counterpropagating laser beams, we have

$$D = cE_R/U_0, \quad (15)$$

where U_0 is the depth of the optical potential and E_R the recoil energy, and the dimensionless parameter c depends on the atomic transition involved.^b For $p \ll 1$, the cooling force Eq. (14) is harmonic, $F(p) \sim -p$, while in the opposite limit, $p \gg 1$, $F(p) \sim -1/p$. It is useful, given the correspondence between Eq. (13a) and overdamped motion in space subject to a force F ,

^bFor atoms in molasses with a $J_g = 1/2 \rightarrow J_e = 3/2$ Zeeman substructure in a lin \perp lin laser configuration $c = 12.3$.⁶ Refs. 5,20,21 give $c = 22$. As pointed out in⁶ different notations are used in the literature.

to define an effective potential

$$V(p) = - \int_0^p F(p) dp = (1/2) \ln(1 + p^2). \quad (16)$$

This potential is asymptotically logarithmic, $V(p) \sim \ln(p)$ when p is large, which has as its consequence various unusual equilibrium and non-equilibrium properties of the momentum distribution.^{20–25} For example the steady state momentum distribution is $W_{eq}(p) \propto \exp[-V(p)/D]$ which has a power law form

$$W_{eq}(p) = \mathcal{N}(1 + p^2)^{-1/2D} \quad (17)$$

where \mathcal{N} is the normalization. Such non-Gaussian behavior was observed in the experiments of Renzoni's group.²¹ For $D < 1/3$, corresponding to shallow optical lattices, the averaged kinetic energy diverges. A similar effect was found experimentally by Walther's group:²² when the depth of the optical lattice is tuned one may observe a gigantic increase of the energy of the system. Of course the energy of a physical system cannot be infinite and this paradox was recently resolved^{23,24} by treating the problem dynamically, revealing that the energy may increase with time but it is never infinite. Of course, when the energy becomes too large, other experimental effects become relevant as well.

While the velocity distribution of the atomic cloud appears to be well understood, the new experiment⁴ demands a theory for the spatial spreading. This will be the focus of this chapter. However, by now the reader might think that laser cooling is an oxymoron. Namely if we get non-Maxwellian distributions in equilibrium, fat tails, and Lévy behavior, where is the thermal state found? The answer, as we understand it, is rather involved. First the equilibrium momentum PDF can be rather narrow in its center, and in that sense the atoms are cold. Further, the divergence of energy happens for low D , so an experimentalist interested in cooling will turn their knobs away from that limit. In fact there is an optimal depth of the optical potential in the sense that it yields the smallest value for the mean kinetic energy of the particles, since the basic energy scale is set by the optical potential depth (see, e.g., Fig. 4 of Ref. 22 and Fig. 2 of Ref. 26). Strictly speaking, however, for all D the equilibrium state is not thermal since the momentum distribution is not Gaussian. Experimentalist intuitively recognize this problem, and hence also use a method called evaporation to reach an ultimate cold state. Evaporation simply means that atoms in the tails, i.e. atoms with high velocities, are a problem for cooling, so they are

allowed by the experimentalist to leave the system. Another mechanism that may lead to a realistic thermal state is internal collisions among the atoms (which will depend of-course on the density). It is believed that such effects will lead the system in the long time limit to thermal equilibrium. However, at least in the experiments briefly surveyed here,^{4,21,22} which take long times on atomic scale (e.g. milliseconds) no hint of thermal Maxwellian equilibrium is found, at least for values of D of interest. Hence it is an important task to map the different phases of the dynamics which are controlled by D . Indeed this system is truly wonderful in the sense that the experimentalist can tune D and hence explore different effects both in and out of equilibrium.

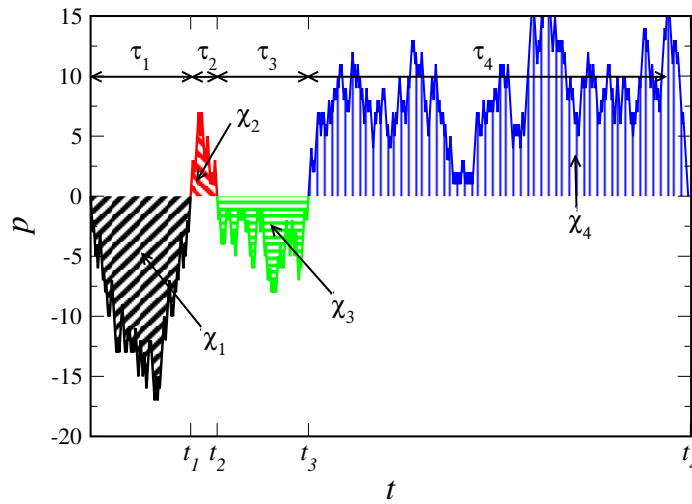


Fig. 3. Schematic presentation of the momentum of the particle versus time. The times between consecutive zero crossings are called the jump durations τ and the shaded area under each excursion are the random flight displacements χ . The τ 's and the χ 's are correlated, since statistically a long jump duration implies a large displacement.

3. From Area under the Bessel excursion to Lévy walks for the packet of atoms

The heart of our analysis is the mapping of the Langevin dynamics to a recurrent set of random walks. The particle along its stochastic path in momentum space crosses $p = 0$ many times when the measurement time

is long. Let $\tau > 0$ be the random time between one crossing event to the next crossing event, and let $-\infty < \chi < \infty$ be the random displacement (for the corresponding τ). As schematically shown in Fig. 3, the process starting at the origin with zero momentum is defined by the sequence of jump durations, $\{\tau_1, \tau_2, \dots\}$ with corresponding displacements $\{\chi_1, \chi_2, \dots\}$, with $\chi_1 \equiv \int_0^{\tau_1} p(\tau) d\tau$, $\chi_2 \equiv \int_{\tau_1}^{\tau_1+\tau_2} p(\tau) d\tau$, etc. The total displacement x at time t is a sum of the individual displacements χ_i . Since the underlying Langevin dynamics is continuous, we need a more precise definition of this process. Let τ be the time it takes the particle with initial momentum p_i to reach $p_f = 0$ for the first time. So τ is the first passage time for the process in momentum space. Eventually we will take $p_i \rightarrow p_f$, see below. Similarly, χ is the displacement of the particle during this flight. Namely by definition χ is the area under the Langevin curve (in momentum space) till the first passage time. The probability density function (PDF) of the displacement χ is denoted $q(\chi)$ and of the jump durations $g(\tau)$. To conclude we see that first passage time statistics, in particular the area swept under the random momentum process $p(\tau)$ until the first passage time, constitute the microscopical random jumps and correlated random waiting times which eventually give the full displacement of the particle.

As shown by Marksteiner, et al. and Lutz,^{6,20} these PDFs exhibit power law behavior

$$g(\tau) \propto \tau^{-\frac{3}{2}-\frac{1}{2D}}, \quad (18a)$$

$$q(\chi) \propto |\chi|^{-\frac{4}{3}-\frac{1}{3D}}, \quad (18b)$$

as a consequence of the logarithmic potential, which makes the diffusion for large enough p only weakly bounded. It is this power-law behavior, with its divergent second moment of the displacement χ for $D > 1/5$, which gives rise to the anomalous statistics for x (measured in the experiment). Notice that taking the limit $D \rightarrow \infty$ in Eq. (18) we get the expected results as given in Eqs. (6) and (11). In this limit, the cooling force $F(p)$ is negligible, the dynamics is governed by the noise in Eq. (13) and so the process $p(t)$ approaches a Brownian motion. This corresponds to atoms emitting a photon in random directions, and hence from the recoil jolts, they are undergoing an unbiased random walk in momentum space (which is the pure heating limit).

Importantly, and previously overlooked, there is a strong correlation between the jump duration τ and the spatial extent of the jumps χ . These correlations are responsible, in particular, for the finiteness of the moments of $P(x, t)$. Physically, such a correlation is obvious, since long jump dura-

tions involve large momenta, which in turn induce a large spatial displacement. The theoretical development starts then from the quantity $\psi(\chi, \tau)$, the joint probability density of $|\chi|$ and τ . From this, we construct a Lévy walk scheme^{27–29} which relates the microscopic information $\psi(\chi, \tau)$ to the atomic packet $P(x, t)$ for large x and t .

4. Scaling Theory for Anomalous Diffusion

We rewrite the joint PDF

$$\psi(\chi, \tau) = \frac{1}{2} g(\tau) p(|\chi| | \tau), \quad (19)$$

where $p(\chi | \tau)$ is the conditional probability to find a jump length of $0 < \chi < \infty$ for a given jump duration τ . The factor $\frac{1}{2}$ accounts for the walks with $\chi < 0$. Numerically we observed that the conditional probability scales at large times like

$$p(\chi | \tau) \approx 2\tau^{-\gamma} B(|\chi|/\tau^\gamma); \quad \gamma = 3/2. \quad (20)$$

$B(\cdot)$ is a scaling function soon to be determined. To analytically obtain the scaling exponent $\gamma = 3/2$ note that $q(\chi) = \int_0^\infty d\tau \psi(\chi, \tau)$, giving

$$q(\chi) \sim \int_{\tau_0}^\infty d\tau \tau^{-\frac{3}{2} - \frac{1}{2D}} \tau^{-\gamma} B\left(\frac{|\chi|}{\tau^\gamma}\right) \propto |\chi|^{-(1 + \frac{1+1/D}{2\gamma})}. \quad (21)$$

Here τ_0 is a time scale after which the long time limit in Eqs. (18) holds and is irrelevant for large χ . Comparing Eq. (21) to Eq. (18b) yields the consistency condition $1 + (1 + 1/D)/(2\gamma) = 4/3 + 1/(3D)$ and hence $\gamma = 3/2$, as we observe in Fig. 4.

We see that the scaling function $B(\cdot)$ in Eq. (20) is similar to the problem of the area under a Brownian excursion. However, now we are confronted with the additional impact of the friction force. The concept of the Brownian excursion needs to be extended to a stochastic curve called the Bessel excursion,³⁰ which corresponds to with the friction force $F(p) = -1/p$. The term Bessel excursion stems from the fact that mathematically speaking, diffusion in momentum space, in the non-regularized potential $\ln(p)$, corresponds to a process called the Bessel process.^{31,32} As with the Brownian excursion, the Bessel excursion is the Langevin path $p(t')$ over the time interval $0 \leq t' \leq \tau$ such that the path starts on $p_i \rightarrow 0$ and ends on the origin, but is *constrained* to stay positive (if $p_i > 0$) or negative (if $p_i < 0$). Brownian excursions are just the $D \rightarrow \infty$ limit of this more general problem. Schematic excursions $p(t)$ are presented in Fig. 3, albeit

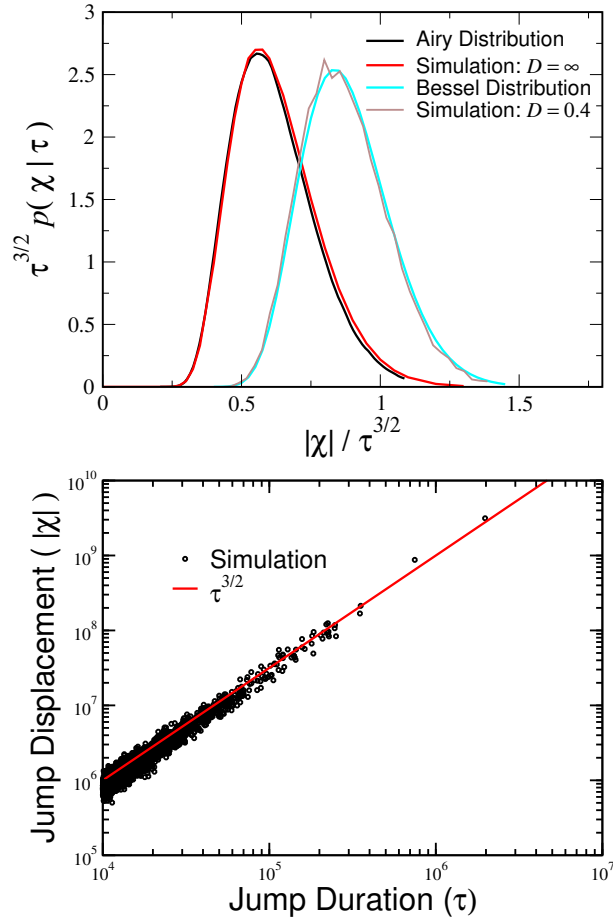


Fig. 4. Lower panel: We plot the flight displacement $|\chi|$ versus the jump duration τ to demonstrate the strong correlations between these two random variables. Here $D = 2/3$ and the line has slope $3/2$ reflecting the $\chi \sim \tau^{3/2}$ scaling discussed in the text. Upper panel: The conditional probability $p(\chi|\tau)$ is described by the Airy distribution^{14,15} when $D \rightarrow \infty$; otherwise by the distribution derived here based on the Feynman-Kac theory, Eq. (24). They describe areas under constrained Brownian (or Bessel) excursions when the cooling force $F(p) = 0$ (or $F(p) \neq 0$) respectively.

there with various excursion times τ . The displacement $\chi = \int_0^\tau p(t')dt'$ is the area under the excursion as shown in Fig. 3.

4.1. Area Under the Bessel Excursion

We briefly outline how to obtain the distribution of the area under the Bessel excursion, namely we find the rather formidable $p(\chi|\tau)$, Eq. (24) below. The main tool we use is a modified Feynman-Kac theory. The original well-known formalism deals with functionals of Brownian motion, while here we deal with functionals of Langevin motion, hence the modification. The Feynman-Kac equation is essentially a Schrödinger equation in real time and is reviewed in Ref. 33. The calculation involves three steps:

- (a) We first find $\tilde{G}(s, p, \tau)$, the Laplace transform with respect to χ of the joint PDF for the positively constrained path to reach p with area χ at time τ , which we denote by $G(\chi, p, t)$.
- (b) Taking the limit of the initial and final momentum $p_i = p \rightarrow 0$, we get $\tilde{p}(s|\tau) = \lim_{p, p_i \rightarrow 0} \tilde{G}(s, p, \tau) / \tilde{G}(s = 0, p, \tau)$; the $\tilde{G}(s = 0, p, \tau)$ denominator yields the correct normalization.
- (c) Finally, using the inverse Laplace transform, we get $p(\chi|t)$.

As mentioned, the main tool we use is the modified Feynman-Kac formalism for functionals of over-damped Langevin paths.^{33,34} For step (a) we solve:

$$\frac{\partial \tilde{G}(s, p, \tau)}{\partial \tau} = [\tilde{L}_{\text{fp}} - sp] \tilde{G}(s, p, \tau), \quad (22)$$

where $\tilde{L}_{\text{fp}} = D(\partial_p)^2 - \partial_p F(p)$ is the Fokker Planck operator. When $F(p) = 0$, Eq. (22) is the celebrated Feynman-Kac equation which is an imaginary-time Schrödinger equation in a linear potential (i.e. the $-sp$ term). We do not provide here a derivation of Eq. (33) but in Sec. 8 provide a derivation of a related equation. The constraint $p > 0$ gives the boundary condition $\tilde{G}(s, p = 0, t) = 0$, i.e., an infinite potential barrier when $p < 0$ in the quantum language. We use the force $F(p) = -1/p$ since we are interested only in the scaling behavior of the problem where large excursions imply that the small p behavior of the force is not important. This assertion can be mathematically justified, but here for the sake of space we will only demonstrate it numerically (see Fig. 4). Solving Eq. (22) and following the recipe (a) - (b) we find

$$\tilde{p}(s|\tau) = \sum_{k=1}^{\infty} 2^{3\nu+1} \Gamma\left(1 + \frac{3}{2}\nu\right) \left(s D^{1/2} \tau^{2/3}\right)^{\nu+2/3} [g'_k(0)]^2 e^{-\tau D^{1/3} \lambda_k s^{2/3}}. \quad (23)$$

Here $Dg_k'' + (g_k/p)' - pg_k = -D\lambda_k g_k$ is the eigenvalue equation which gives the eigenvalues λ_k and eigenstates $g_k(p)$ which are normalized according $\int_0^\infty [g_k(p)]^2 p^{1/D} dp = 1$. A detailed mathematical derivation will soon be published.³⁵

It is easy to tabulate the eigenvalues λ_k and the slopes on the origin $g_k'(p=0)$ with standard numerically exact techniques. With this information and the inverse Laplace transform we find the solution in terms of generalized hypergeometric functions

$$p(\chi|\tau) = -\frac{\Gamma(1 + \frac{3\nu}{2})}{4\pi\chi} \left(\frac{4D^{1/3}\tau}{\chi^{2/3}}\right)^{1+3\nu/2} \times \sum_k [g_k'(0)]^2 \left[{}_2F_2\left(\frac{4}{3} + \frac{\nu}{2}, \frac{5}{6} + \frac{\nu}{2}; \frac{1}{3}, \frac{2}{3}; -\frac{4D\lambda_k^3\tau^3}{27\chi^2}\right) c_0 \right. \\ \left. - {}_2F_2\left(\frac{7}{6} + \frac{\nu}{2}, \frac{5}{3} + \frac{\nu}{2}; \frac{2}{3}, \frac{4}{3}; -\frac{4D\lambda_k^3\tau^3}{27\chi^2}\right) c_1 \right. \\ \left. + {}_2F_2\left(2 + \frac{\nu}{2}, \frac{3}{2} + \frac{\nu}{2}; \frac{4}{3}, \frac{5}{3}; -\frac{4D\lambda_k^3\tau^3}{27\chi^2}\right) \frac{c_2}{2} \right], \quad (24)$$

where

$$c_j = \left(\frac{D^{1/3}\lambda_k\tau}{\chi^{2/3}}\right)^j \Gamma\left(\frac{5+2j}{3} + \nu\right) \sin\left(\pi\frac{2+2j+3\nu}{3}\right) \quad j = 0 \dots 2 \quad (25)$$

and the summation is over the eigenvalues. Here we have introduced the parameter

$$\nu \equiv \frac{1+D}{3D} \quad (26)$$

which will turn out to play a crucial role in the dynamics. Notice the $\chi \sim \tau^{3/2}$ scaling which proves the scaling hypothesis, Eq. (20). To compare with numerical simulations, we evaluate this function truncating the sum beyond some k , since for fixed x the terms decay rapidly in k . The Langevin simulations were performed by mapping the problem onto a biased random walk in momentum space, with momentum spacing $\delta p = 0.1$.

In Fig. 4, we present $p(\chi|\tau)$ obtained from numerical simulations, showing that it perfectly matches our theory on Bessel excursions without fitting. Our theory and simulations show that the areas under the Brownian and Bessel excursions share the same $\chi \sim \tau^{3/2}$ scaling behavior. In both cases, $p(\chi|\tau)$ falls off rapidly for large $|\chi|$, ensuring finite moments of this distribution, which will prove important later. When $D \gg 1$, the Bessel and the

Brownian excursions coincide, since then the force $F(p)$ plays a vanishing role, as can be shown directly from Eq. (24). The Bessel excursion PDF for finite D is compared with the limiting Airy distribution in Fig. 4, where it is seen that the Bessel excursions are pushed further away from the origin. The $-1/p$ force implies that trajectories not crossing the origin in $(0, \tau)$ are typically further away from the origin, compared with the free Brownian particle, since trajectories close to the origin are more likely to cross it, due to the attractive force.

4.2. Coupled Continuous Time Random Walk Theory from First Passage Time Statistics

The next step is to relate the first passage time properties of the underlying Langevin process in momentum space, namely the joint distribution of the area under the Bessel excursion and the first passage time, with the spreading of the density $P(x, t)$. Given our scaling solution for $p(\chi|t)$, and $g(\tau)$ which is considered in detail in Ref. 35 (see also Appendix here) and hence $\psi(\chi, t)$, we construct a theory for $P(x, t)$ using tools developed in the random walk community.²⁷ As soon detailed, one first obtains a Montroll-Weiss⁹ type of equation for the Fourier-Laplace transform of $P(x, t)$, $\tilde{P}(k, u)$, in terms of $\tilde{\psi}(k, u)$, the Fourier-Laplace transform of the joint PDF $\psi(\chi, \tau)$:

$$\tilde{P}(k, u) = \frac{\Psi(k, u)}{1 - \tilde{\psi}(k, u)}. \quad (27)$$

Here, $\Psi(k, u)$ is the Fourier-Laplace transform of $\tau^{-3/2}B(|\chi|/\tau^{3/2})[1 - \int_0^t \psi(\tau)d\tau]$. The last step is then to invert Eq. (27) back to the x, t domain.

To derive Eq. (27) we present a formalism which relates the joint distribution

$$\psi(\chi, \tau) = g(\tau)\tau^{-3/2}B(|\chi|/\tau^{3/2}) \quad (28)$$

with $P(x, t)$ ($B(\cdot)$ is given in Eqs. (20,24)). Define $\eta_s(x, t)dtdx$ as the probability that the particle crossed the momentum state $p = 0$ for the s^{th} time in the time interval $(t, t + dt)$ and that the particle's position was $(x, x + dx)$. This probability is related to the probability of the $s-1$ crossing according to

$$\eta_s(x, t) = \int_{-\infty}^{\infty} dv_{3/2} \int_0^{\infty} d\tau \eta_{s-1}(x - v_{3/2}\tau^{3/2}, t - \tau) B(|v_{3/2}|) g(\tau) \quad (29)$$

where we changed the variable of integration to $v_{3/2} \equiv \chi/\tau^{3/2}$. Now the process is described by a sequence of jump durations τ_1, τ_2, \dots and the corresponding generalized velocities $v_{3/2}(1), v_{3/2}(2), \dots$ (with units $[x]/[t^{3/2}]$). The displacements in the s th interval is: $\chi_s = v_{3/2}(s)[\tau_s]^{3/2}$. The advantage of the representation of the problem in terms of the pair of microscopic stochastic variables $\tau, v_{3/2}$ (instead of the correlated pair τ, χ) is clear from Eq. (29): we may treat $v_{3/2}$ and τ as independent random variables whose corresponding PDFs are $g(\tau)$ and $B(v_{3/2})$ respectively. The initial condition $x = 0$ at time $t = 0$ implies $\eta_0(x, t) = \delta(x)\delta(t)$. Let $P(x, t)$ be the probability of finding the particle in $(x, x + dx)$ at time t , which is found according to

$$P(x, t) = \sum_{s=0}^{\infty} \int_{-\infty}^{\infty} dv_{3/2} \int_0^{\infty} d\tau \eta_s(x - v_{3/2}\tau^{3/2}, t - \tau) B(|v_{3/2}|) W(\tau). \quad (30)$$

since for a time series with s intervals, the last jump event took place at $t - \tau$ and in the time period $(t - \tau, t)$ the particle did not cross the momentum origin (hence the survival probability $W(\tau) = 1 - \int_0^{\tau} g(\tau) d\tau$). The summation in Eq. (30) is a sum of all possible realizations with s returns to the momentum origin $p_f = 0$.

As usual,^{9,27} we consider the problem in Laplace-Fourier space where $t \rightarrow u$ and $x \rightarrow k$. Eq. (29) then translates to

$$\tilde{\eta}_s(k, u) = \tilde{\eta}_{s-1}(k, u) \tilde{\psi}(k, u). \quad (31)$$

Here the tildes refer to the Fourier-Laplace transforms, and we have used Eq. (20) to write that $\psi(\chi, \tau) = g(\tau)\tau^{-3/2}B(|\chi|/\tau^{3/2})$. Hence, summing the Fourier-Laplace transform of Eq. (30) using Eq. (31), we get the Montroll-Weiss Eq. (27).

The Montroll-Weiss equation is widely used in applications of the random walk. This equation holds since the underlying dynamics is Markovian, namely each time the process $p(t)$ crosses zero, the process is renewed. However, there is a subtle point behind our approach, which makes it different. Since the trajectories are continuous, the number of zero crossings s is infinite within any finite time interval $(0, t)$, and for a particle starting with $p = 0$. In contrast in usual continuous time random walk theories the number of renewals is always finite, and it increases with time. The functions entering the right hand side of Eq. (27) still depend on the initial momentum we assign to the particle $\pm p_i$ immediately after each zero crossing (if we use a grid in a numerical simulation this is handled automatically). We

still must take the limit $p_i \rightarrow 0$ and show that our final expression will give sensible results in that regularized limit (see also Ref. 35).

5. The Lévy phase

We now explain why Lévy statistics describes the diffusion profile $P(x, t)$ when $1/5 < D < 1$, provided that x is not too large. The key idea is that, for x 's which are large, but not extremely large, the problem decouples, and $\tilde{\psi}(k, u)$ can be expressed as a product of the Fourier transform of $q(\chi)$, $\tilde{q}(k)$ and the Laplace transform of $g(\tau)$, $\tilde{g}(u)$. This is valid as long as $x \ll t^{3/2}$, since otherwise paths where $\chi \sim t^{3/2}$ are relevant, for which the correlations are strong, as we have seen. The long-time, large- x behavior of $P(x, t)$ in the decoupled regime is then governed by the small- k behavior of $\tilde{q}(k)$ and the small u behavior of $\tilde{g}(u)$. When the second moment of $q(\chi)$ diverges, i.e. for $D > 1/5$, the small- k behavior of $\tilde{q}(k)$ is determined by the large- χ asymptotics of $q(\chi)$ as given in Eq. (20), $q(\chi) \sim x_*^\nu/|\chi|^{1+\nu}$. When the first moment of τ is finite, i.e. for $D < 1$, the small- u behavior of $\tilde{g}(u)$ is governed by the first moment, $\langle \tau \rangle$. From these follow the small- k , small- u behavior of $\tilde{P}(k, u)$:

$$\tilde{P}(k, u) \sim \frac{1}{u + K_\nu |k|^\nu} \quad (32)$$

where $K_\nu = \pi x_*^\nu / (\langle \tau \rangle \Gamma(1 + \nu) \sin \frac{\pi\nu}{2})$ (see some details in Appendix A).

Both x_*^ν and $\langle \tau \rangle$ can be calculated (see Appendix A and Ref. 35) via appropriate backward Fokker-Planck equations. They both vanish as the magnitude of the initial momentum of the walk goes to zero, but their ratio has a finite limit, so that K_ν , upon returning to dimensionfull units, is

$$K_\nu = \frac{\sqrt{\pi}(3\nu - 1)^{\nu-1} \Gamma(\frac{3\nu-1}{2})}{\Gamma(\frac{3\nu-2}{2}) 3^{2\nu-1} [\Gamma(\nu)]^2 \sin(\frac{\pi\nu}{2})} \left(\frac{p_c}{m}\right)^\nu (\bar{\alpha})^{-\nu+1}. \quad (33)$$

$\tilde{P}(k, u)$, as given in Eq. (32), is in fact precisely the symmetric Lévy distribution in Laplace-Fourier space with index ν , whose (x, t) representation is (see Eq. (B17) of Ref. 36)

$$P(x, t) \sim \frac{1}{(K_\nu t)^{1/\nu}} L_{\nu,0} \left[\frac{x}{(K_\nu t^{1/\nu})} \right]. \quad (34)$$

The properties of the Lévy function $L_{\nu,0}(\cdot)$ are well-known, and the solution in time for the spatial Fourier transform is $P(k, t) = \exp(-K_\nu t |k|^\nu)$ with $2/3 < \nu < 2$. This distribution is the solution of the fractional diffusion

equation, Eq. (4), with $\beta = 1$ and an initial distribution located at the origin. This justifies the use of Eq. (4) in Ref. 4 for $1/5 < D < 1$ and provides ν and K_ν in terms of the experimental parameters. We can verify this behavior in simulations, as shown in Fig. 3, where we see excellent agreement to our theoretical prediction, Eqs. (34) and (33), without any fitting.

The fractional diffusion equation, Eq. 4, has the following meaning and connection to the underlying random walk. We re-express Eq. (32) as $u\tilde{P}(k, u) - 1 = -K_\nu |k|^\nu \tilde{P}(k, u)$. Recalling⁹ that the Fourier space representation of the Weyl-Rietz fractional derivative, ∇^ν , is $-|k|^\nu$ and that $u\tilde{P}(k, u) - 1$ is the representation of the time derivative in Laplace space for δ -function initial conditions centered at the origin, we see that in fact $P(x, t)$ satisfies the fractional diffusion equation, Eq. (4), with $\beta = 1$.

Fig. 5 (b) also illustrates the cutoff on the Lévy distribution, which is found at distances $x \sim t^{3/2}$, as can be seen also from Fig 5(c). Beyond this length scale, the density falls off rapidly (Fig. 5(c)). This, as noted above, is the result of the correlation between χ and τ , as there are essentially no walks with a displacement greater than of order $t^{3/2}$. This cutoff ensures the finiteness of the mean square displacement, using the power law tail of the Lévy PDF $L_\nu(x) \sim x^{-(1+\nu)}$ and the cutoff we get:

$$\langle x^2 \rangle \simeq \int_0^{t^{3/2}} t^{-(1/\nu)} (x/t^{1/\nu})^{-(1+\nu)} x^2 dx \sim t^{4-3\nu/2},$$

for $2/3 < \nu < 2$, in agreement with rigorous results of Ref. 37 (where the prefactor is also computed). As noted in the introduction, if we rely on the fractional diffusion equation, Eq. (4), naively, we get $\langle x^2 \rangle = \infty$. Thus the fractional equation must be used with care, realizing its limitations in the statistical description of the moments of the distribution and its tails.

6. Richardson Phase

When the average jump duration, $\langle \tau \rangle$, diverges, i.e., for $D > 1$, the dynamics of $P(x, t)$ enters a new phase. Since the Levy index ν approaches $2/3$ as D approaches 1, x scales like $t^{3/2}$ in the limit. Due to the correlations, x cannot grow faster than this, so in this regime, $P(x, t) \sim t^{-3/2} h(x/t^{3/2})$. This scaling is that of free diffusion, namely momentum diffuses like $p \sim t^{1/2}$ and hence the time integral over the momentum scales like $x \sim t^{3/2}$. Indeed, in the absence of the logarithmic potential, namely in the limit $D \gg 1$

Transport and the first passage time problem with application to cold atoms in optical traps 21

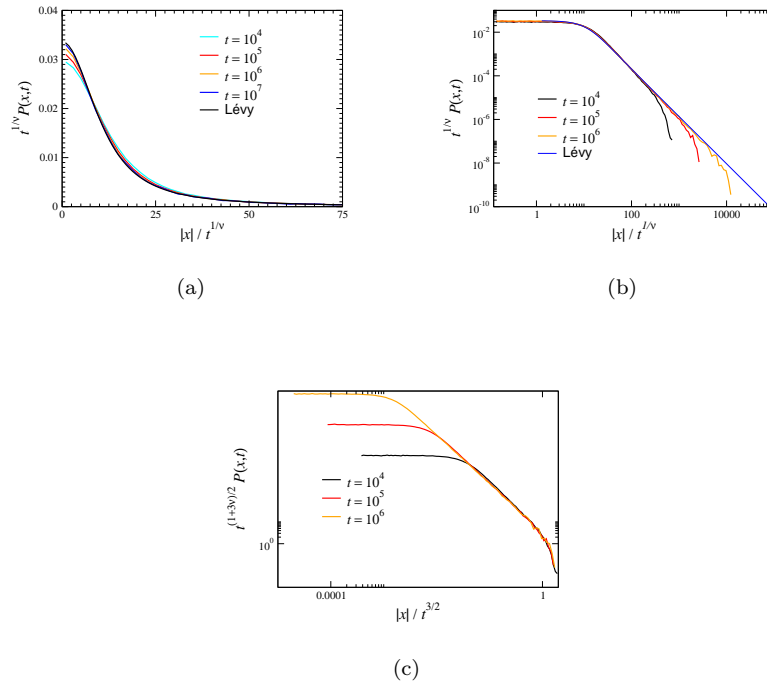


Fig. 5. (a) $t^{1/\nu}P(|x|,t)$ versus $|x|/t^{1/\nu}$ for $D = 2/5$, i.e. $\nu = 7/6$. The theory, i.e., the Lévy PDF Eq. (34) along with K_ν , Eq. (33), perfectly matches simulations without fitting. (b) Same data in log-log scale. Notice the cutoff for large x which is due to the coupling between jump lengths and jump durations, making $x > t^{3/2}$ extremely improbable. (c) $t^{(1+3\nu)/2}P(|x|,t)$ versus $|x|/t^{3/2}$ for $D = 2/5$, showing the crossover from power-law to Gaussian behavior at $|x| \sim t^{3/2}$. This cutoff ensures the finiteness of the mean square displacement of the underlying spreading of the packet of atoms.

Eq. (13) gives

$$P(x,t) \sim \sqrt{\frac{3}{4\pi Dt^3}} \exp\left[-\frac{3x^2}{4Dt^3}\right]. \quad (35)$$

This limit describes the Obukhov model for a tracer particle path in turbulence, where the velocity follows a simple Brownian motion.^{38,39} These scaling properties are related to Kolmogorov's theory of 1941 (see Eq. (3) in Ref. 39) and to Richardson diffusion^{37,40} $\langle x^2 \rangle \sim t^3$. Eq. (35) is valid when the optical potential depth is small since $D \rightarrow \infty$ when $U_0 \rightarrow 0$. This

limit should be taken with care, as the observation time must be made large before considering the limit of weak potential. In the opposite scenario, i.e. $U_0 \rightarrow 0$ before $t \rightarrow \infty$, we expect ballistic motion, $|x| \sim t$, since then the optical lattice has not had time to make itself felt.⁴

7. Relation between first passage times and diffusivity

When the variance of χ is finite, namely $\nu > 2$, we get normal diffusion so that $P(x, t)$ is a Gaussian. In that case the spatio-temporal distribution of jump times and jump lengths decouples $\psi(\chi, \tau) \simeq q(\chi)g(\tau)$. The mean square displacement $\langle x^2 \rangle \sim 2K_2 t$ and the diffusion constant is

$$K_2 = \lim_{\epsilon \rightarrow 0} \frac{\langle \chi^2 \rangle}{2\langle \tau \rangle}. \quad (36)$$

This equation relates the first passage time properties of the momentum process and the spatial diffusivity and it has the structure of the famous Einstein relation, relating the variance of jump sizes and the average time to make a jump, with a diffusion constant. However here we are dealing with a special limit, namely $\langle \tau \rangle$ is the average time it takes for a particle with initial momentum $p_i = \pm\epsilon$ to reach $p = 0$ for the first time. This average first passage time vanishes in the limit of $\epsilon \rightarrow 0$. The variance of χ , is $\langle \chi^2 \rangle = \int_{-\infty}^{\infty} \chi^2 q(\chi) d\chi$ namely the variance of the area under the random first passage process $p(t')$ till its first return to $p = 0$, and it too vanishes in the limit $\epsilon \rightarrow 0$. Notice that here χ may be either positive or negative (see Fig. 3) and its mean is zero (since the particle may start on $p_i = \pm\epsilon$) with equal probability since the force $F(p)$ is zero on $p = 0$. Of-course from symmetry $F(p) = -F(-p)$, so it suffices to consider χ for say positive areas only.

The calculation of $\langle \tau \rangle$ and $\langle \chi^2 \rangle$ is based on backward Fokker-Planck equations Eqs. (A.1,A.3) (see further details in Ref. 35) and we find

$$K_2 = \frac{1}{D\mathcal{Z}} \int_{-\infty}^{\infty} dp e^{V(p)/D} \left[\int_p^{\infty} dp' e^{-V(p')/D} p' \right]^2, \quad (37)$$

and $\mathcal{Z} = \int_{-\infty}^{\infty} \exp[-V(p)/D] dp$. This equation was derived previously using a different approach in Ref. 41. The coefficient K_2 diverges as $D \rightarrow 1/5$ from below indicating the transition to the superdiffusive phase. A sharp increase in the diffusion coefficient of an atomic cloud as the laser intensity reaches a critical value was detected experimentally by Hodapp et al.,⁴¹ which could be the fingerprint of the transition from Gaussian to the Lévy

phase. We see that the Green-Kubo formula, Eq. (3), is not the only way to calculate the diffusion constant. For Markovian processes, with non-linear friction, using Eq. (36) and calculating the first passage time properties is an alternative. In the normal diffusion case, the Green-Kubo formalism is so successful that the existence of an alternate method is only of academic interest. However, as shown throughout this current work, calculations of first passage time properties of the velocity process are very useful for the unraveling of the anomalous spatial diffusion properties of the system, where we cannot use the standard Green-Kubo formalism nor the Gaussian central limit theorem. See further work on a generalized Green-Kubo formalism and non-stationary momentum correlation functions in Ref. 26.

8. Equation for the distribution of the area swept by a particle until its first passage

We briefly outline the derivation of the equation for the PDF of the area $\chi = \int_0^t p(t')dt'$ under the stochastic process $p(t) \geq 0$ which starts on $p_i > 0$ until it reaches $p = 0$ for the first time, so that t is the first passage time. The PDF $q(|\chi|)$ has a Laplace $\chi \rightarrow s$ transform which we call $Q(s, p_i)$ (here $\chi > 0$ the extension to negative χ being trivial). The equation for this quantity is

$$D \frac{d^2 Q}{dp_i^2} + F(p_i) \frac{dQ}{dp_i} - sp_i Q = 0. \quad (38)$$

For simplicity and for conciseness we consider the case $F(p) = 0$, so $p(t)$ is undergoing Brownian motion without bias. By definition $\chi_{p_i} = \int_0^t p(t')dt'$ so

$$Q(s, p_i) = \langle \exp[-s \int_0^t p(t')dt'] \rangle_{p_i} \quad (39)$$

where t is the first passage time. The starting point is denoted by the subscript. Now we consider the process $p(t)$ as a random walk on a lattice with probability 1/2 to jump from $p(t) \rightarrow p(t) + \delta p$ or $p(t) \rightarrow p(t) - \delta p$, so δp is the lattice spacing. The constant times between these jumps is δt and we consider the limit $\delta p \rightarrow 0$ and $\delta t \rightarrow 0$ while keeping $D = (\delta p)^2 / 2\delta t$ finite, this being the Brownian limit.

A particle starting with p_i at time $t = 0$ can either have momentum $p_i - \delta p$ at time δt with probability one half, or $p_i + \delta p$ with the same

probability. From the definition of χ_{p_i} and for a particle starting with p_i we have

$$\chi_{p_i} = \begin{cases} p_i \delta t + \chi_{p_i - \delta p} & \text{Prob } 1/2 \\ p_i \delta t + \chi_{p_i + \delta p} & \text{Prob } 1/2. \end{cases} \quad (40)$$

The first case corresponds to a particle initially jumping down in p , $p_i \rightarrow p_i - \delta p$ while the second case is for a particle jumping up. The term $p_i \delta t$ stems from the displacement during the interval δt , and the remaining term (either χ_{p_i} or $\chi_{p_i + 2\delta p}$ is the displacement for a new process which starts either with $p_i - \delta p$ or $p_i + \delta p$). Eq. (40) is now used to find

$$\langle \exp(-s\chi_{p_i}) \rangle = \frac{1}{2} \sum_{\sigma=\pm 1} \langle \exp[-s(p_i \delta t - s\chi_{p_i + \sigma \delta p})] \rangle. \quad (41)$$

Expanding the right hand side of Eq. (41) to second order in δp and first order in δt , and inserting these expansions in Eq. (41), using $D = (\delta p)^2/2\delta t$, we get Eq. (38). For $F(p_i) \neq 0$ a similar approach is used though now weights on the jumping probabilities must be implemented (see similar expansions in Refs. 13,34). The boundary condition $Q(s, p_i)|_{p_i=0} = 1$ is used since a particle starting on $p_i \rightarrow 0$ will immediately reach $p = 0$ and then the PDF of χ is a delta function centered on zero, so the Laplace transform of this delta function $Q(s, 0)$ is equal to unity. We use eq. (38) in Appendix A (and in more detail in Ref. 35) to derive the long tail of $q(\chi)$ and from it K_ν .

9. Discussion of the experiment

Our work shows a rich phase diagram of the dynamics, with two transition points. For deep wells, $D < 1/5$, the diffusion is Gaussian, while for $1/5 < D < 1$ we have Lévy statistics, and for $D > 1$ the Richardson-Obukhov scaling $x \sim t^{3/2}$ is found. So far, experiments detected a Gaussian phase and an anomalous one. A transition to Richardson-Obukhov scaling has not yet been detected. Sagi et al. ⁴ clearly demonstrated that changing the optical potential depth modifies the anomalous exponents in the Lévy spreading packet. However, the experiment showed at most ballistic behavior, with the spreading exponent δ , defined by $x \sim t^\delta$, always less than unity. This might be related to our observation that to go beyond ballistic motion, $\delta > 1$, one must take the measurement time to be very long. A more serious problem is that, in the experimental fitting of the diffusion front to the Lévy propagator, an additional exponent was introduced⁴ to

describe the time dependence of the full width at half maximum. In contrast, our semi-classical theory shows that a single exponent ν is needed within the Lévy scaling regime $1/5 < D < 1$, with the spreading exponent $\delta = 1/\nu$. This might be related to the cutoff of the tails of Lévy PDF which demands that the fitting be performed in the central part of the atomic cloud. On the other hand we cannot rule out other physical effects not included in the semiclassical model. For example it would be very interesting to simulate the system with quantum Monte Carlo simulations, though we note that these are not trivial in the $|x| \sim t^{3/2}$ regime since the usual simulation procedure introduces a cutoff on momentum, which may give rise to an artificial ballistic motion. Further, the experiment suffers from leakage of particles, which could be crucial, while our theory assumes conservation of the number of particles. Another effect our theory does not address is the Doppler cooling which may serve as a cutoff at long time scales (see some discussion on this in²⁶). Thus while there is some tantalizing points of contact between the theory and experiment, full agreement is yet far away.

10. Summary

Usually first passage times are derived from a random diffusive processes. Here our goal was a bit different. We use first passage time statistics to derive the spatial diffusivity of the atomic cloud. We revealed also general relations between first passage times and the normal diffusion constant K_2 . Since the latter, through linear response, is in many cases related to the mobility, we see that analysis of first passage time problems in momentum space can be very helpful. For this analysis, we need not only distributions of first passage times (which was a topic thoroughly investigated previously) but also relatively new tools (at least in physics), namely the distributions of areas under the Langevin curve till the random first arrival, and the analysis of the area under positive excursion curves like the Bessel excursion with fixed time interval. The area under the Brownian excursion, e.g. the Airy distribution, is found to be useful in a special limit ($D \rightarrow \infty$) which is encouraging since this mathematical object had very little to do with physical behavior up until the recent works in the field. The rich phase diagram, i.e. Normal, Lévy, Richardson diffusions, together with the divergence of the diffusion constant close to the transition, revealed by the semi-classical approach used here, point to interesting physics, though many open questions and challenges both experimental and theoretical remain

open with respect to the dynamics and thermodynamics of laser cooled atoms.

Acknowledgements

This work was supported by the Israel Science Foundation. We thank Andreas Dechant, Eric Lutz, Nir Davidson, Yoav Sagi, and Satja Majumdar for discussions. EB thanks the Free University of Berlin for hospitality during the preparation of the manuscript.

Appendix A.

In this appendix we derive the small k , small u behavior of $\tilde{\psi}$. We first note²⁸ that for $u^{3/2} \ll k \ll 1$, $D < 1$, we can approximate $\tilde{\psi}$ by its decoupled form, $\tilde{\psi}(k, u) \sim \tilde{g}(u)\tilde{q}(k)$. For small u , since g is a probability distribution, we have $\tilde{g}(u) \sim 1 - u\langle\tau\rangle$, as long as the first moment exists. This first moment satisfies the backward Fokker-Planck equation⁴²

$$D \frac{d^2 \langle\tau\rangle}{dp_i^2} + F(p_i) \frac{d\langle\tau\rangle}{dp_i} = -1 \quad (\text{A.1})$$

and the small p_i limit of the solution is:

$$\langle\tau\rangle \sim \frac{p_i}{D} \int_0^\infty e^{-V(p)} dp = \frac{p_i \sqrt{\pi} \Gamma\left(\frac{3\nu-2}{2}\right)}{2D\Gamma\left(\frac{3\nu-1}{2}\right)} \quad (\text{A.2})$$

For small k behavior of $\tilde{q}(k)$, given that the second moment diverges, we have $\tilde{q}(k) \sim 1 - \pi x_*^\nu |k|^\nu / (\Gamma(1+\nu) \sin \frac{\pi\nu}{2})$. The length scale x_* governing the decay of $q(\chi)$ can in principle be determined from the scaling function B , but it is easier to get it directly from another backward Fokker-Planck equation for the Laplace transform of $q(\chi)$, $Q(s, p_i)$, where we have made explicit the dependence on the initial momentum $p_i > 0$ (so $\chi > 0$):

$$D \frac{d^2 Q}{dp_i^2} + F(p_i) \frac{dQ}{dp_i} - s p_i Q = 0. \quad (\text{A.3})$$

From this, we derive the small p_i , small s behavior: $Q(s, p_i) \sim 1 - p_i \Gamma(1 - \nu)(3\nu - 1)^\nu s^\nu / (\Gamma(\nu) 3^{2\nu-1})$, which in turn yields

$$x_*^\nu \sim p_i \frac{\nu(3\nu - 1)^\nu}{2 \cdot 3^{2\nu-1} \Gamma(\nu)} \quad (\text{A.4})$$

where the $1/2$ prefactor stems from equal consideration of positive and negative excursions. Putting these two results together, we have

$$\tilde{\psi}(k, u) \approx 1 - \langle\tau\rangle u - x_*^\nu |k|^\nu \dots \quad (\text{A.5})$$

Transport and the first passage time problem with application to cold atoms in optical traps 27

To leading order, we may approximate $\Psi(k, u) \sim \Psi(0, u) \sim 1/\langle\tau\rangle$, which, together with Eq. (A.5), gives us Eq. (32).

References

1. C. N. Cohen-Tannoudji and W. D. Phillips, New mechanisms for laser cooling, *Phys. Today* **43**(10), 33–40 (1990).
2. F. Bardou, J. P. Bouchaud, A. Aspect, and C. Cohen-Tannoudji, *Lévy Statistics and Laser Cooling*. Cambridge Univ. Press, Cambridge (2002).
3. C. N. Cohen-Tannoudji, [free to read] nobel lecture: Manipulating atoms with photons, *Rev. Mod. Phys.* **70**(3), 707–719 (1998).
4. Y. Sagi, M. Brook, I. Almog, and N. Davidson, Observation of anomalous diffusion and fractional self-similarity in one dimension, *Phys. Rev. Lett.* **108**(9), 093002 (2012).
5. Y. Castin, J. Dalibard, and C. Cohen-Tannoudji. The limits of Sisyphus cooling. In eds. L. Moi, S. Gozzini, C. Gabbanini, E. Arimondo, and F. Strumia, *Light Induced Kinetic Effects on Atoms, Ions and Molecules*, ETS Editrice, Pisa (1991).
6. S. Marksteiner, K. Ellinger, and P. Zoller, Anomalous diffusion and levy walks in optical lattices, *Phys. Rev. A* **53**(5), 3409–3430 (1996).
7. A. I. Saichev and G. M. Zaslavsky, Fractional kinetic equations: solutions and applications, *Chaos* **7**(4), 753–764 (1997).
8. R. Metzler, E. Barkai, and J. Klafter, Deriving fractional Fokker-Planck equations from a generalized master equation, *Europhys. Lett.* **46**(4), 431–436 (1999).
9. R. Metzler and J. Klafter, The random walk’s guide to anomalous diffusion: a fractional dynamics approach, *Phys. Rep.* **339**(1), 1–77 (2000).
10. J. Klafter, M. F. Shlesinger, and G. Zumofen, Beyond brownian motion, *Physics Today* **49**(2), 33–39 (1996).
11. E. Schrödinger, The theory of drop and rise tests on brownian motion particles, *Physik. Z.* **16**, 289–295 (1915).
12. S. Redner, *A Guide to First-Passage Processes*. Cambridge Univ. Press, Cambridge (2001).
13. S. N. Majumdar and M. J. Kearney, On the area under a continuous time Brownian motion till its first-passage time, *J. Phys. A: Mathematical and General* **38**(19), 4097–4104 (2005).
14. S. N. Majumdar and A. Comtet, Exact maximal height distribution of fluctuating interfaces, *Phys. Rev. Lett.* **92**(22), 225501 (2004).
15. S. N. Majumdar and A. Comtet, Airy distribution function: From the area under a brownian excursion to the maximal height of fluctuating interfaces, *J. Stat. Phys.* **119**(3–4), 777–826 (2005).
16. D. A. Darling, On the supremum of a certain gaussian process, *Ann. Probab.* **11**(3), 803–806 (1983).
17. G. Louchard, Kac formula, Lévy local time and Brownian excursion, *J. Appl. Probab.* **21**(3), 479–499 (1984).

18. L. Takács, A Bernoulli excursion and its various applications, *Adv. Appl. Probab.* **23**(3), 557–585 (1991).
19. M. Abramowitz and I. A. Stegun, eds., *Handbook of Mathematical Functions*. Dover, New York (1972).
20. E. Lutz, Power-law tail distributions and nonergodicity, *Phys. Rev. Lett.* **93**(19), 190602 (2004).
21. P. Douglas, S. Bergamini, and F. Renzoni, Tunable Tsallis distributions in dissipative optical lattices, *Phys. Rev. Lett.* **96**(11), 110601 (2006).
22. H. Katori, S. Schlipf, and H. Walther, Anomalous dynamics of a single ion in an optical lattice, *Phys. Rev. Lett.* **79**(12), 2221–2224 (1997).
23. D. A. Kessler and E. Barkai, Infinite invariant densities for anomalous diffusion in optical lattices and other logarithmic potentials, *Phys. Rev. Lett.* **105**(12), 120602 (2010).
24. A. Dechant, E. Lutz, E. Barkai, and D. A. Kessler, Solution of the Fokker-Planck equation with a logarithmic potential, *J. Stat. Phys.* **145**(6), 1524–1545 (2011).
25. O. Hirschberg, D. Mukamel, and G. M. Schütz, Approach to equilibrium of diffusion in a logarithmic potential, *Phys. Rev. E* **84**(4), 041111 (2011).
26. A. Dechant, E. Lutz, D. A. Kessler, and E. Barkai, Generalized green-kubo relation and application to superdiffusion in optical lattices, *submitted*.
27. J. Klafter, A. Blumen, and M. F. Shlesinger, Stochastic pathway to anomalous diffusion, *Phys. Rev. A* **35**(7), 3081–3085 (1987).
28. A. Blumen, G. Zumofen, and J. Klafter, Transport aspects in anomalous diffusion – Lévy walks, *Phys. Rev. A* **40**(7), 3964–3974 (1989).
29. E. Barkai and J. Klafter, Anomalous diffusion in the strong scattering limit: A Lévy walk approach. In eds. S. Benkadda and G. M. Zaslavsky, *Chaos, Kinetics and Nonlinear Dynamics in Fluids and Plasmas: Proceedings of a workshop held in Carry-Le Rouet, France 16-21 June 1997*, vol. 511, *Lecture Notes in Physics*, pp. 373–394, Springer, Berlin (1998).
30. Y. Hu and Z. Shi, Extreme lengths in Brownian and Bessel excursions, *Bernoulli* **3**(4), 387–402 (1997).
31. A. J. Bray, Random walks in logarithmic and power-law potentials, nonuniversal persistence, and vortex dynamics in the two-dimensional XY model, *Phys. Rev. E* **62**(1), 103–112 (2000).
32. G. Schehr and P. Le Doussal, Extreme value statistics from the real space renormalization group: Brownian motion, Bessel processes and continuous time random walks, *J. Stat. Mech.: Theory and Expt.* **2010**(1), P01009 (2010).
33. S. N. Majumdar, Brownian functionals in physics and computer science, *Current Sci.* **89**(12), 2076–2092 (2005).
34. S. Carmi and E. Barkai, Fractional Feynman-Kac equation for weak ergodicity breaking, *Phys. Rev. E* **84**(6), 061104 (2011).
35. D. A. Kessler and E. Barkai, From the area under the Bessel excursion to Lévy walks in optical lattices, (*in preparation*).
36. J. P. Bouchaud and A. Georges, Anomalous diffusion in disordered media: Statistical mechanisms, models and physical applications, *Phys. Rep.* **195**

*Transport and the first passage time problem with application to cold atoms in optical traps*29

- (4–5), 127–293 (1990).
37. A. Dechant, E. Lutz, D. A. Kessler, and E. Barkai, Fluctuations of time averages for langevin dynamics in a binding force field, *Phys. Rev. Lett.* **107** (24), 240603 (2011).
 38. A. M. Obukhov, Description of turbulence in terms of lagrangian variable, *Adv. Geophys.* **6**, 113–116 (1959).
 39. A. Baule and R. Friedrich, Investigation of a generalized obukhov model for turbulence, *Phys. Lett. A.* **350**(3–4), 167–173 (2006).
 40. L. F. Richardson, Atmospheric diffusion shown on a distance-neighbour graph, *Proc. Roy. Soc. Lond. A.* **110**(756), 709–737 (1926).
 41. T. W. Hodapp, C. Gerz, C. Furtlehner, C. I. Westbrook, W. D. Phillips, and J. Dalibard, Three-dimensional spatial diffusion in optical molasses, *Appl. Phys. B.* **60**(2–3), 135–143 (1995).
 42. C. W. Gardiner, *Handbook of Stochastic Methods for Physics, Chemistry and the Natural Sciences*, 3 edn. Springer, Berlin (2003).